The FEBS Journal

FEBS PRESS science publishing by scientists

Post-translational incorporation of 3,4-dihydroxyphenylalanine into the C terminus of α-tubulin in living cells

Yanela M. Dentesano[1,†], Yanina Ditamo[1,†], Cristian Hansen[2], Carlos A. Arce[1] and Carlos Gaston Bisig[1]

1 Centro de Investigaciones en Química Biológica de Córdoba (CIQUIBIC), UNC-CONICET, Departamento de Química Biológica, Facultad de Ciencias Químicas, Universidad Nacional de Córdoba, Argentina
2 LACE S.A., Córdoba, Argentina

Keywords
Dopa incorporation; Dopa-tubulin; microtubules; Tyr-tubulin; α-tubulin C terminus

Correspondence
C. G. Bisig, CIQUIBIC-CONICET, Depto. Quimica Biologica, Fac. de Ciencias Quimicas, Pabellon Argentina, Universidad Nacional de Cordoba, Cordoba, CP 5000, Argentina
Tel/Fax: +54 351 535 3850
E-mail: bisig@fcq.unc.edu.ar

[†]These authors contributed equally to this study and should be considered co-first authors.

(Received 14 June 2017, revised 7 November 2017, accepted 11 January 2018)

doi:10.1111/febs.14386

The C-terminal tyrosine (Tyr) of the α-tubulin chain is subjected to post-translational removal and readdition in a process termed the "detyrosination/tyrosination cycle". We showed in previous studies using soluble rat brain extracts that L-3,4-dihydroxyphenylalanine (L-Dopa) is incorporated into the same site as Tyr. We now demonstrate that L-Dopa incorporation into tubulin also occurs in living cells. We detected such incorporation by determining the "tyrosination state" of tubulin before and after incubation of cells in the presence of L-Dopa. The presence of a tubulin isospecies following L-Dopa incubation that was not recognized by antibodies specific to Tyr- and deTyr-tubulin was presumed to reflect formation of Dopa-tubulin. L-Dopa was identified by HPLC as the C-terminal compound bound to α-tubulin. L-Dopa incorporation into tubulin was observed in Neuro 2A cells and several other cell lines, and was not due to *de novo* protein biosynthesis. Dopa-tubulin had microtubule-forming capability similar to that of Tyr- and deTyr-tubulin. L-Dopa incorporation into tubulin did not notably alter cell viability, morphology, or proliferation rate. CAD cells (a neuron-like cell line derived from mouse brain) are easily cultured under differentiating and nondifferentiating conditions, and can be treated with L-Dopa. Treatment of CAD cells with L-Dopa and consequent increase in L-Dopa-tubulin resulted in reduction of microtubule dynamics in neurite-like processes.

Introduction

Tubulin, the major protein constituent of microtubules, is subjected following its biosynthesis to removal and readdition of the tyrosine (Tyr) residue encoded at the C terminus of the α-chain. This post-translational modification of tubulin is termed the "detyrosination/tyrosination cycle" [1,2]. Following removal of terminal Tyr by tubulin carboxypeptidase (TCP), Tyr is readded to the C terminus by tubulin tyrosine ligase (TTL). Glutamic acid is exposed after Tyr removal; thus, two tubulin species are involved in this cycle: Tyr-tubulin and deTyr-tubulin. Other enzymes [3,4] remove the C-terminal glutamic acid from deTyr-tubulin, generating a third tubulin species termed Δ2-tubulin (because it lacks the two C-terminal amino acids of the α-chain), which cannot re-enter the cycle [5,6]. Thus, the so-called "tyrosination state" of tubulin reflects the proportion of each species present in a given soluble preparation, cell, or tissue. Tubulin

Abbreviations
CPA, pancreatic carboxypeptidase A; deTyr-tubulin, tubulin lacking Tyr at the C terminus of the α-chain, such that glutamic acid is exposed; Dopa-tubulin, tubulin in which Dopa replaces Tyr at the C terminus of the α-chain; L-Dopa, L-3,4-dihydroxyphenylalanine; TTL, tubulin tyrosine ligase; Tyr-tubulin, tubulin having Tyr at the C terminus of the α-chain.

was the first protein reported to undergo this type of post-translational modification, and until recently was considered to be the only substrate of TTL. A quantitatively minor protein, EB1 (one of the microtubule plus-end tracking proteins), was recently reported to undergo detyrosination/tyrosination in a particular highly specialized cell type [7]. However, EB1 evidently does not undergo detyrosination in brain or neuronal cells [8]. The physiological role of the detyrosination/tyrosination cycle remains to be fully clarified, although association of deTyr-tubulin and Tyr-tubulin with particular proteins and molecular motors has been reported [2,9–13]. In a series of studies, we have examined the role of the cycle by altering tubulin tyrosination state through replacement of C-terminal Tyr with Tyr analogs, and measuring cell physiological effects. Using soluble rat brain extracts, we showed that several Tyr analogs can be incorporated into the α-tubulin C terminus: phenylalanine (Phe) [14], L-3,4-dihydroxyphenylalanine (L-Dopa) [15], aza-Tyr [16], and 3-NO_2-Tyr [17]. Incorporation of Phe into tubulin altered certain physiological parameters in neuron-like CAD cells, suggesting that this might be the cause of observed neuronal dysfunction in phenylketonuric patients [14]. Possible incorporation of L-Dopa into tubulin is of particular interest because the most frequent therapeutic treatment for Parkinson's disease involves prolonged exposure of patients to high-concentration L-Dopa. We speculated that a neuronal dysfunction (Levodopa-induced dyskinesia) sometimes observed in patients treated in this way may involve incorporation of L-Dopa into the α-tubulin C terminus. By using direct and indirect procedures, we demonstrated post-translational incorporation of L-Dopa into the α-tubulin C terminus of various types of cells. Dopa-tubulin was assembled into and disassembled from microtubules *in vitro* similarly to Tyr-tubulin. L-Dopa incorporation into the α-tubulin C terminus was associated with a reduction in microtubule dynamics at growth cone-like structure of CAD cells.

Results

Presence of Dopa-tubulin revealed by analyzing the tyrosination state of tubulin

Because we were unable to obtain a reliable Ab specific to Dopa-tubulin for detecting and monitoring its presence, we developed an alternative method based on the analysis of the tyrosination state of tubulin. Our rationale was that incubation of a tubulin preparation in the presence of L-Dopa under incorporating conditions results in the appearance of a new tubulin species (presumably Dopa-tubulin) that is not recognized by anti-deTyr- or anti-Tyr-tubulin Abs, and consequent alteration of the tyrosination state of tubulin relative to a corresponding preparation without L-Dopa incorporation. This hypothesis was tested by incubating soluble rat brain preparations in the presence or absence (control experiment) of CPA to remove C-terminal Tyr from tubulin, thus increasing the amount of acceptor tubulin molecules for subsequent incorporation of amino acids. After this, a CPA inhibitor (CPi) was added to inhibit CPA activity, and identical aliquots were incorporated with L-Tyr or L-Dopa and then subjected to western blotting using anti-Tyr-, anti-deTyr-, anti-Δ2-, and anti-total-tubulin Abs. We determined optical density (O.D.) of each band, and tyrosination state of brain extract samples before and after CPA treatment. O.D. determined for various tubulin species were standardized relative to total-tubulin. None of the treatments resulted in modification of Δ2-tubulin (Fig. 1A,B). CPA treatment resulted in a striking (> 80%) decrease in Tyr-tubulin and a corresponding increase in deTyr-tubulin. Following L-Tyr incorporation into CPA-treated preparation, the band corresponding to Tyr-tubulin increased to pre-CPA-treatment level, and deTyr-tubulin declined accordingly. In contrast, the aliquot subjected to L-Dopa incorporation, although it contained a much lower amount of deTyr-tubulin (because of partial conversion into other tubulin species), did not show a compensating increase in Tyr-tubulin. The reduced content of deTyr- and Tyr-tubulin in the sample incubated with L-Dopa was presumed to result from formation of Dopa-tubulin (which was not revealed by any of the Abs used).

Dopa-tubulin is assembled into and disassembled from microtubules *in vitro* to the same degree as Tyr-tubulin

[^{14}C]Dopa-tubulin and [^{3}H]Tyr-tubulin were prepared *in vitro* as described previously [15,17], mixed immediately with fresh rat brain soluble extract, incubated for 10, 20, or 30 min under microtubule polymerization conditions, and centrifuged. [^{14}C] and [^{3}H] radioactivity bound to protein was measured in supernatant (nonassembled tubulin) and pellet (assembled tubulin) fractions (Fig. 2A). Radioactivity amount, as a function of time, increased in pellet fraction and decreased in supernatant fraction, suggesting a gradual increase in microtubule mass. Degree of assembly was similar for [^{14}C]Dopa-tubulin and [^{3}H]Tyr-tubulin at any given time, indicating that the two isoforms have the

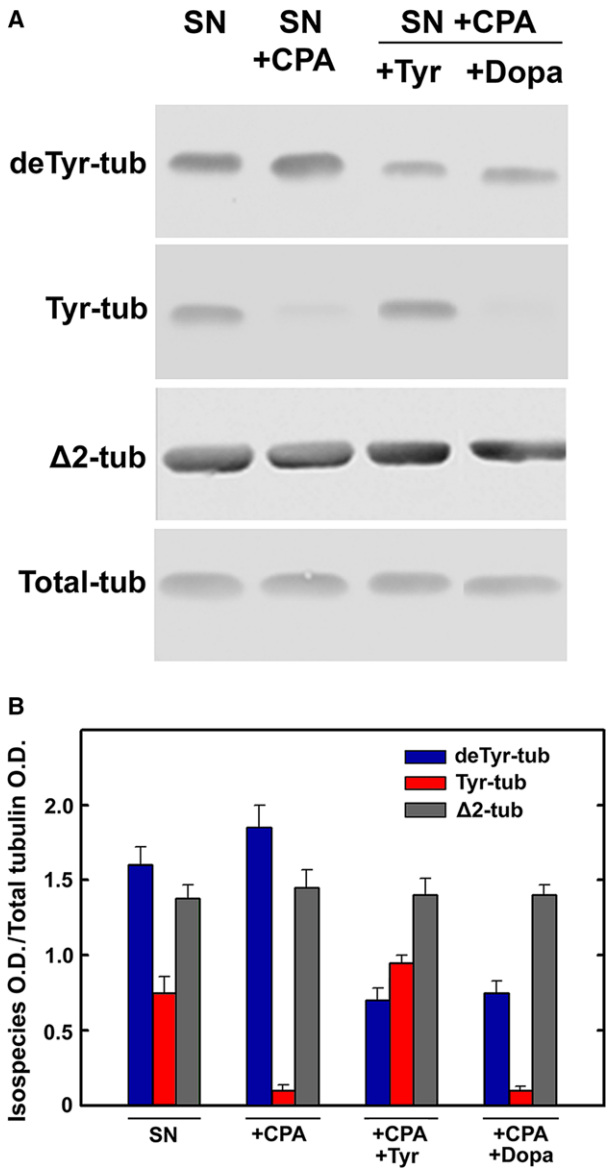

Fig. 1. *In vitro* incorporation of L-Dopa into tubulin. Fresh rat brain soluble extract (SN) was incubated at 37 °C for 10 min with 10 μg·mL^{-1} CPA, filtered through a Sephadex G-25 column (SN + CPA), and added with 50 μg·mL^{-1} CPI (a CPA inhibitor). The preparation was incubated for 30 min at 37 °C to incorporate L-Tyr (+Tyr) or L-Dopa (+Dopa) into endogenous tubulin under the conditions described in Materials and methods. Equal aliquots were analyzed by western blotting using Abs specific to deTyr-tubulin (deTyr-tub), Tyr-tubulin (Tyr-tub), Δ2-tubulin (Δ2-tub), and total-tubulin (Total-tub). (A) Western blot from a typical experiment. (B) O.D. of bands corresponding to three tubulin isospecies, standardized relative to total-tubulin. O.D. corresponding to Δ2-tubulin bands was divided by four, and then used for calculation of the ratio Δ2-tubulin O.D./total-tubulin O.D. Data are expressed as mean ± SD from four independent experiments.

same capability to assemble into microtubules under *in vitro* conditions.

Under similar experimental conditions, Tyr- and Dopa-tubulin showed the same capability to disassemble from microtubules. [^{14}C]Dopa-tubulin and [^{3}H]Tyr-tubulin were prepared and mixed immediately with fresh rat brain soluble extract. Two identical samples were incubated for 30 min to form microtubules. One sample (control) was then immediately centrifuged. A second sample was diluted with nine volumes of buffer, incubated at 0 °C for 30 min to induce disassembly of microtubules, and centrifuged. [^{3}H]Tyr-tubulin amount in the second sample was ~ 45% of that in the control sample (Fig. 2B). Thus, cold/dilution treatment induced disassembly of > 50% of microtubules. Similar results were obtained for [^{14}C]Dopa-tubulin. These findings indicate similar disassembly capability for the two tubulin molecules (Dopa- and Tyr-tubulin) found in microtubules.

L-Dopa is post-translationally incorporated into tubulin in a concentration-dependent manner without affecting cell viability

Incorporation of L-Dopa into tubulin of cultured Neuro 2A cells was assessed as described previously [18], with preincubation in mHBSS alone for 30 min to reduce the amount of intracellular Tyr. Cells were then incubated in mHBSS in the absence or presence of 500 μM L-Dopa or 150 μM Tyr for 3 h. Immunofluorescence analysis showed that Tyr incubation resulted in very weak deTyr-tubulin staining (Fig. 3A), presumably because of transformation of deTyr- to Tyr-tubulin. Tyr/deTyr immunofluorescence intensity ratio was higher in this case (1.49 ± 0.21) than that of control cells (1.09 ± 0.11). L-Dopa incubation also resulted in very weak deTyr-tubulin staining, and an immunofluorescence intensity ratio (1.72 ± 0.16) higher than that of control cells. However, the low deTyr-tubulin level in this case cannot be attributed to the transformation of deTyr- to Tyr-tubulin. Instead, we hypothesized that it was due to the incorporation of L-Dopa into tubulin. More precise quantitation was achieved by analysis of tubulin tyrosination state from western blots, as described in Materials and methods. Δ2-tubulin was not analyzed because it is not present in Neuro 2A cells. Incubation in the presence of L-Dopa (+Dopa) resulted in a reduction of deTyr- and/or Tyr-tubulin relative to control cells, such that the sum of these two isospecies did not account for total-tubulin (Fig. 3B,C). The difference was attributed to the presence of Dopa-tubulin. The percentage of Dopa-tubulin formed was estimated based on absolute amounts of

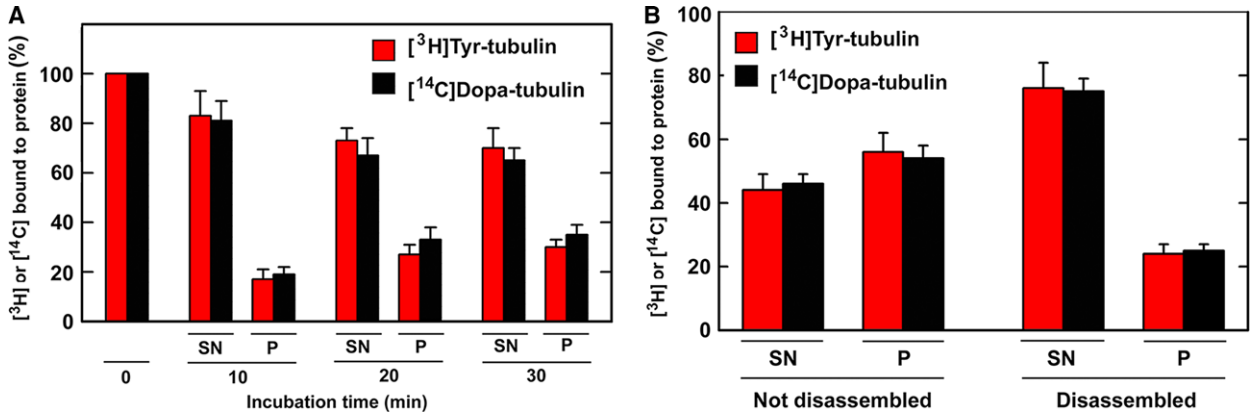

Fig. 2. Capability of Dopa-tubulin to assemble into and to disassemble from microtubules. (A) Fresh soluble rat brain fraction was divided into two identical portions, which were incubated for incorporation of [^{14}C]Dopa and [^{3}H]Tyr (respectively) into tubulin. Each fraction was immediately passed through Sephadex G-25 column to eliminate unincorporated amino acid, mixed gently with three volumes of fresh supernatant fraction (not passed through Sephadex), and incubated at 37 °C under microtubule assembly conditions. Aliquots were removed at 0, 10, 20, and 30 min and centrifuged at 100 000 *g* for 15 min. [^{14}C] and [^{3}H] radioactivity bound to hot TCA-insoluble material was determined in supernatant and resuspended pellet fractions. Values are expressed as percentage [^{14}C] and [^{3}H] in a given fraction relative to the sum of radioactivity bound to assembled (P) and nonassembled (SN) tubulin fractions. (B) Assembled [^{14}C] and [^{3}H] tubulin preparations were obtained after 30 min of incubation under microtubule assembly conditions as described in (A). One aliquot was centrifuged to separate P and SN tubulin fractions. Another aliquot was diluted with nine volumes of assembly buffer and incubated at 0 °C for 30 min. SN and P fractions were simultaneously separated by centrifugation (2–4 °C for 20 min), then subjected to measurement of [^{14}C] and [^{3}H] radioactivity bound to hot TCA-insoluble material. Data are expressed as percentage [^{14}C] and [^{3}H] in each fraction relative to the sum of radioactivity bound to P and SN fractions.

deTyr-, Tyr-, and total-tubulin in western blots and the respective standard curves for each of the tubulin species, as we described previously [14]. Dopa-tubulin was estimated to comprise 38 ± 6% of total-tubulin following incubation of cells with 500 μM L-Dopa for 3 h (data not shown). In cells incubated with increasing concentrations of L-Dopa, Tyr-tubulin level remained constant (or was slightly reduced), while deTyr-tubulin level declined gradually (Fig. 4A,B), indicating that L-Dopa incorporation into the α-tubulin C terminus is concentration-dependent.

L-Dopa incorporation into tubulin was not blocked by cycloheximide (Fig. 4C,D). Thus, the presence of L-Dopa in the C terminus presumably does not result from *de novo* biosynthesis but rather via a post-translational mechanism, perhaps TTL activity.

Viability of cells incubated for 3 h with L-Dopa did not differ from that of control cells (Fig 4E). The same was true for cells incubated for 3 h with L-Dopa and then for 24 h without L-Dopa (Fig. 4E).

Identification and quantitation of the C-terminal amino acid of α-tubulin in L-Dopa-treated cells

To confirm incorporation of L-Dopa into the α-tubulin C terminus, we used HPLC coupled with electrochemical detector to identify the amino acid released by CPA from tubulin of Neuro 2A cells incubated for 3 h in the presence or absence of 500 μM L-Dopa. Cells were subjected to SDS/PAGE, transferred to nitrocellulose sheet, and the portion of the sheet containing the band corresponding to tubulin was cut out and treated with CPA to release the C-terminal amino acid [19]. The chromatogram of authentic L-Dopa (0.02 nmol) used for identification and quantitation is shown in Fig. 5A, and that of a sample of the amino acid removed by CPA from 0.227 nmol tubulin (quantitated by western blotting with pure brain tubulin sample as standard) is shown in Fig. 5B. The main peak coincided with that of standard L-Dopa. L-Dopa was detected in L-Dopa-treated cells (Fig. 5B), but not in control cells (Fig. 5C). By comparison of the area of the peak in Fig. 5B (10 317 $mAU \cdot s^{-1}$) with that of the L-Dopa standard in Fig. 5A (3055 $mAU \cdot s^{-1}$), we calculated that the peak in B corresponds to 0.067 nmol L-Dopa. We thus estimated that 29.5% of tubulin contained L-Dopa as the C-terminal amino acid. This value is close to the value (~38%) obtained from the method based on analysis of the tyrosination state of tubulin as illustrated in Fig. 3.

L-Dopa is incorporated into the α-tubulin C terminus in various cell types

Incorporation of L-Dopa into tubulin under the above conditions was assayed in five cell lines (Neuro 2A,

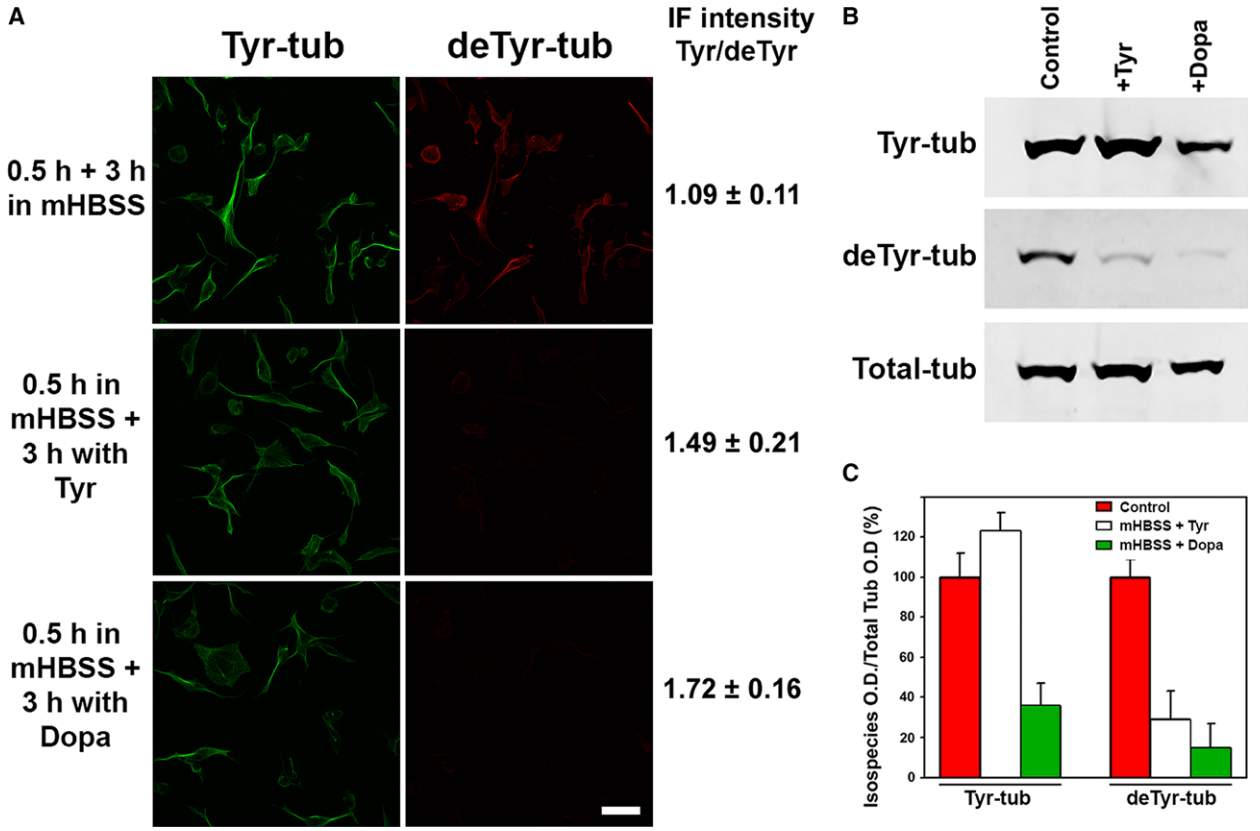

Fig. 3. Incorporation of L-Dopa into tubulin. Neuro 2A cells were cultured as described in Materials and methods, medium was replaced by mHBSS, incubation continued 30 min at 37 °C, medium was replaced by fresh mHBSS containing 500 μM L-Dopa (+Dopa), 150 μM L-Tyr (+Tyr), or neither (Control), and incubation continued 3 h. Cells were then placed on coverslips and subjected to double immunofluorescence using Abs specific to Tyr-tubulin (Tyr-tub) and deTyr-tubulin (deTyr-tub). Cells remaining on dishes were dissolved with Laemmli sample buffer and subjected to western blotting with Abs specific to Tyr-tub, deTyr-tub, and total-tubulin (Total-tub). (A) Immunofluorescence images of Tyr-tub (green) and deTyr-tub (red). Total immunofluorescence intensity of each field was measured using Fiji. Tyr/deTyr ratio is shown at right (mean ± SD from three independent experiments). Images are from a typical experiment. (B) Western blotting of cells remaining on dishes. Images are from a typical experiment. (C) O.D. values of bands from three experiments similar to that shown in (B) were measured, and values for deTyr- and Tyr-tub were standardized relative to Total-tub. Data are expressed as mean ± SD. Scale bar: 50 μm.

C6, CAD, CHO, COS). L-Dopa incubation resulted in reduced levels of deTyr- and/or Tyr-tubulin in each of the cell lines (Fig. 6A,B), indicating that Dopa-tubulin formation is not exclusive to Neuro 2A cells. CAD cells are of particular interest in that besides their capability to incorporate L-Dopa into tubulin, they actively proliferate when incubated in the presence of serum, and differentiate into neuron-like morphology (including several markers typical of functional neurons) in the absence of serum [20,21]. After 2 days incubation in the absence of serum, CAD cells acquired a neuron-like morphology (Fig. 7A). At this stage, incubation of cells with 500 μM L-Dopa for 3 h resulted in reduced proportions of Tyr- and deTyr-tubulin relative to total-tubulin, indicating significant production of Dopa-tubulin (Fig. 7B).

L-Dopa treatment reduces microtubule dynamics

We used three techniques to evaluate effects of L-Dopa treatment on microtubule dynamics: (a) measurement of microtubule depolymerization rate following nocodazole treatment; (b) fluorescence recovery after photobleaching (FRAP) analysis of GFP-tubulin-expressing cells [14]; (c) analysis of microtubule dynamics by visualization of fluorescent "comets" at the growing microtubule plus-ends [22–24] in EB3-EGFP transfected cells. Western blotting was used in each case to confirm that incubation of cells with L-Dopa resulted in its efficient incorporation into tubulin. Nocodazole treatment resulted in slower microtubule depolymerization rate in cells preincubated with L-Dopa than in control cells (Fig. 8A,B). For FRAP

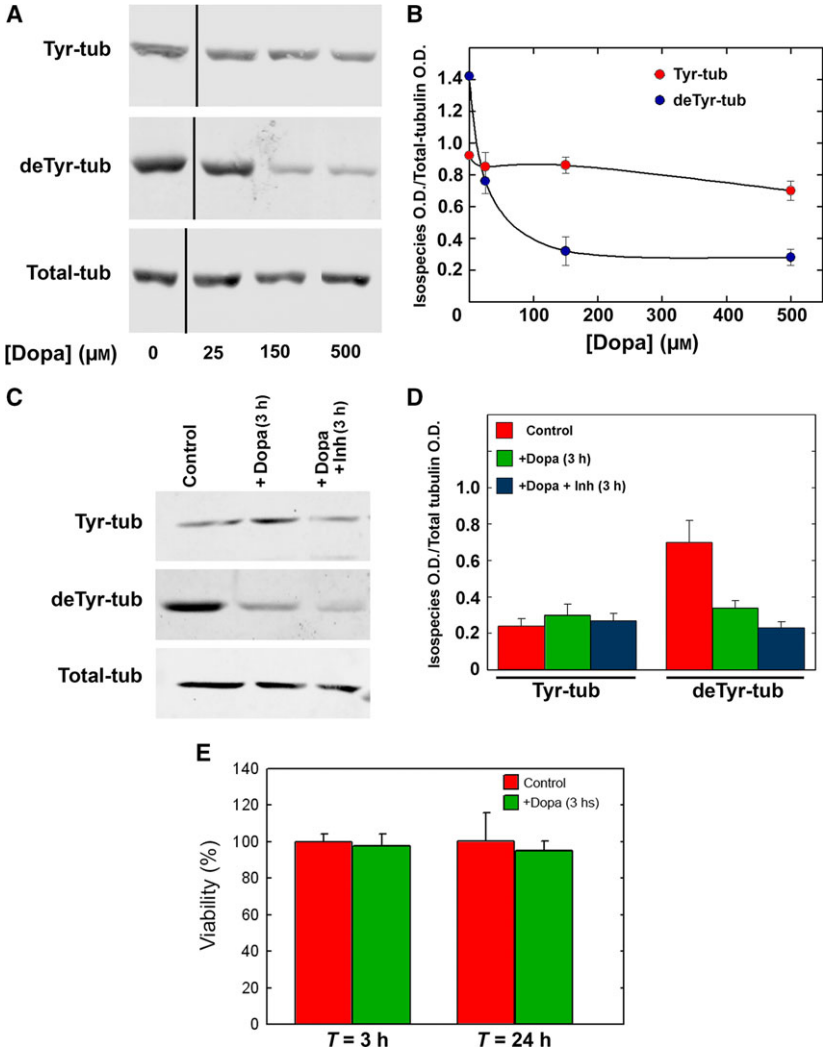

Fig. 4. L-Dopa is post-translationally incorporated into tubulin in a concentration-dependent manner without affecting cell viability. (A) Cultured Neuro 2A cells were preincubated with mHBSS for 30 min at 37 °C, medium was replaced with mHBSS containing the indicated concentrations of L-Dopa, and incubation continued for 3 h. Cells were harvested and subjected to western blotting and immunostaining with anti-Tyr- (Tyr-tub), anti-deTyr- (deTyr-tub), and anti-total-tubulin (Total-tub) Abs to evaluate L-Dopa incorporation through analysis of tyrosination state. The samples were run on the same gel from which intervening nonrelevant lanes were cropped. (B) Quantitation of Tyr-tub and deTyr-tub based on O.D./Total-tub O.D. Data are expressed as mean ± SD from three independent experiments. (C) Cells were cultured as described in (A), and in the presence or absence of 100 μM cycloheximide. Cells were analyzed by western blotting using specific Abs to evaluate tubulin tyrosination state. Images from a typical experiment are shown. (D) O.D. of bands from four independent experiments identical to that shown in C were measured and O.D. ratios of Tyr-tub and deTyr-Tub relative to Total-tub were calculated and expressed as mean ± SD. (E) Determination of cell viability. Cells were cultured as described in (A), incubated 3 h with or without L-Dopa, then either immediately or 24 h later incubated in DMEM/F12 medium for 24 h, and subjected to MTT assay as described in Materials and methods. Absorbance was measured at 490 nm. Number of cells in each treatment group is expressed as the percentage (± SD) relative to the number of cells treated with the vehicle alone. Experiments were performed in triplicate.

analysis, GFP-tubulin-transfected cells were incubated under differentiating conditions for 72 h, and then with 500 μM L-Dopa for 1 h. Selected areas of growth cone-like structures were photobleached, and fluorescence recovery was measured as described in Materials and methods. Fluorescence recovery half-life time ($t_{0.5}$) in control cells was 283 ± 95 s, indicating a high level of microtubule dynamics (Fig. 8C,D; Movie S1). In contrast, $t_{0.5}$ in L-Dopa-treated cells was > 600 s (Fig. 8C,D; Movie S2), indicating a much lower level of microtubule dynamics. In cells preincubated with 10 μM taxol (microtubule-stabilizing agent), no

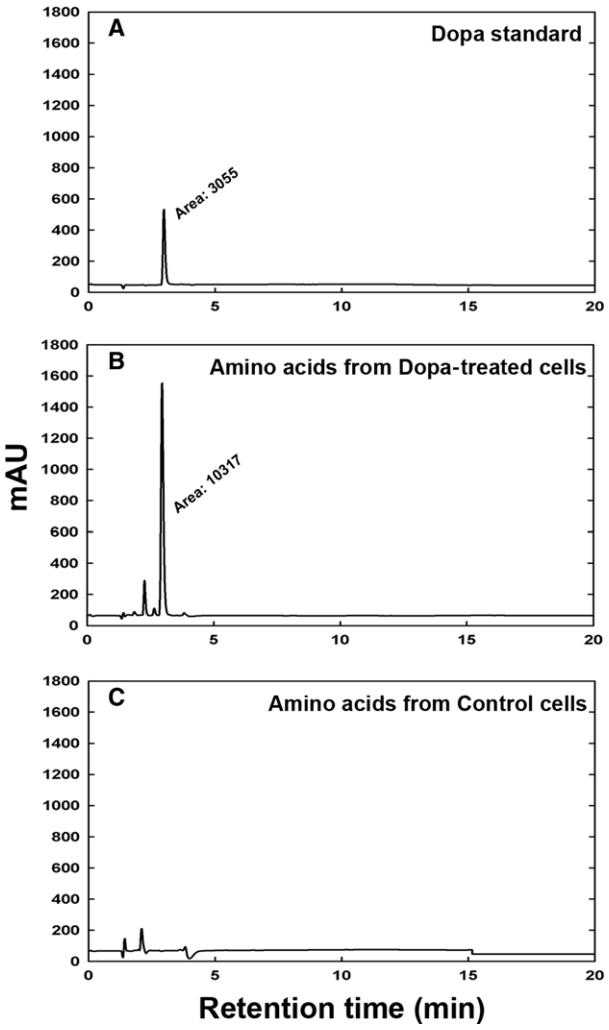

Fig. 5. Identification and quantitation of the C-terminal amino acid of α-tubulin in L-Dopa-treated cells. Neuro 2A cells were incubated in mHBSS with or without 500 μM L-Dopa for 3 h, and then harvested in Laemmli buffer. Proteins were subjected to SDS/PAGE and transferred to nitrocellulose sheet. The nitrocellulose strip containing the tubulin band was cut out, treated with CPA to remove C-terminal residues from tubulin, and the removed amino acids were identified and quantitated by HPLC as described in Materials and methods. Tubulin was quantitated by comparison of western blots with corresponding pure tubulin standard. (A) Chromatogram of L-Dopa standard (0.02 nmol). (B) Chromatogram of amino acids released by CPA from 0.227 nmol tubulin corresponding to L-Dopa treated cells. (C) Chromatogram of amino acids released by CPA from 0.250 nmol tubulin corresponding to control cells.

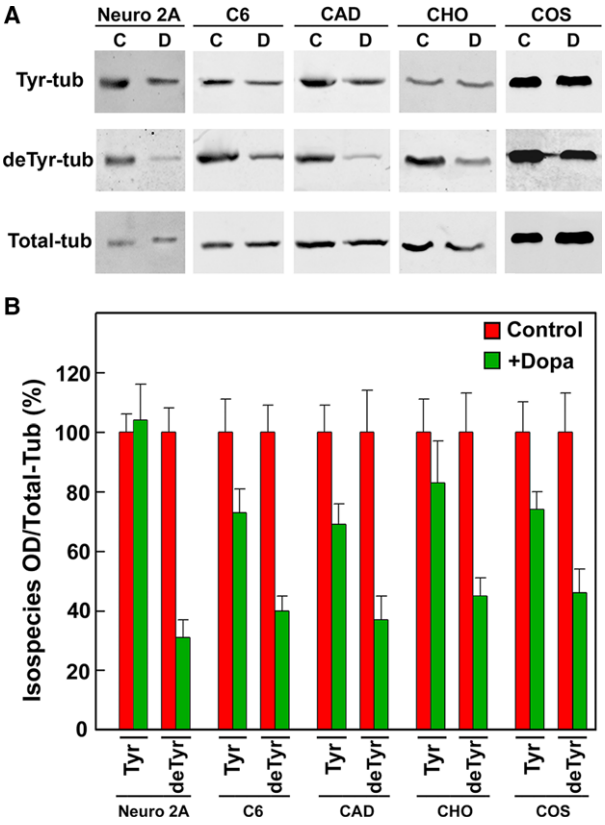

Fig. 6. Incorporation of L-Dopa into tubulin in several cell types. (A) Cultured Neuro 2A, C6, CAD (undifferentiated), CHO, and COS cells were preincubated in mHBSS for 30 min at 37 °C, medium was replaced with mHBSS containing 500 μM L-Dopa (+Dopa) or no addition (Control), and incubation continued 3 h. Identical samples were subjected to western blotting and stained on different lanes using Abs specific to Tyr-, deTyr- and Total-tub. Typical blots for each cell type are shown. (B) For each cell type, O.D. values of bands from experiments identical to that shown in (A) were measured. O.D. ratios of Tyr- and deTyr-tub relative to Total-tub in the Controls were chosen as 100% and the ratio values corresponding to L-Dopa-treated cells were expressed as a percentage relative to the value of the corresponding Control. Data shown for each cell type are mean ± SD from three independent experiments.

fluorescence recovery was observed after photobleaching (Fig. 8C,D; Movie S3). For technique (c) as described above, we transfected cells with plus-end-tracking human EB3 fused to EGFP, and incubated them with or without L-Dopa. EB3 comets [23,25] in L-Dopa-treated cells were significantly shorter (0.62 ± 0.06 μm) than those in control cells (1.02 ± 0.11 μm) (Fig. 9A,B). Images were taken at 3-s intervals. Microtubule instantaneous growth velocity was calculated by superimposing two images separated by 6 s (e.g., image #3 and image #5), and measuring the displacement of the comet during that 6-s period. Mean growth velocity for L-Dopa-treated cells (7 $\mu m \cdot min^{-1}$) was significantly less than that for control cells (11 $\mu m \cdot min^{-1}$) (Fig. 9A,C). Taxol-treated cells had only a few static, short comets (not shown). These findings, taken together, clearly demonstrate

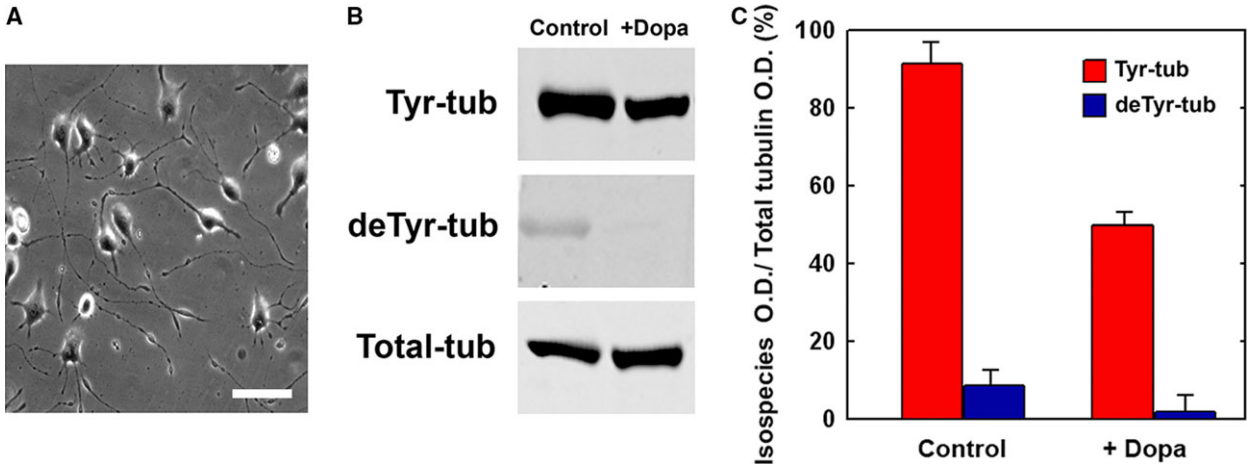

Fig. 7. Incorporation of L-Dopa into tubulin of differentiated CAD cells. CAD cells were cultured for 48 h under differentiating conditions (absence of FBS). Differentiated cells were preincubated in mHBSS for 30 min, medium was replaced by mHBSS containing 500 μM L-Dopa (+Dopa) or vehicle alone (Control), and incubation continued for 3 h. Cells were visualized by microscopy and photographed (A), and analyzed by western blotting (B) using Abs specific to Tyr-, deTyr-, and Total-tub. (C) O.D. values of bands were measured, and O.D. ratios of Tyr- and deTyr-tub relative to Total-tub were expressed as percentage relative to value of Control. Data shown are mean ± SD from three independent experiments. Scale bar: 50 μm.

that L-Dopa treatment of CAD cells reduced microtubule dynamics.

Discussion

Many years ago, we described a post-translational modification of tubulin whereby the C terminus of its α-chain can be tyrosinated or detyrosinated, both *in vitro* and *in vivo*. We demonstrated also that certain tyrosine analogs can replace tyrosine, and that L-Dopa can be incorporated into tubulin in soluble rat brain extracts [26]. In the present study, we used cultured cells to study the incorporation of L-Dopa into the α-tubulin C terminus. [^{3}H]Tyr and [^{14}C]Dopa were useful for labeling of tubulin in *in vitro* experiments (Fig. 2). On the other hand, attempts to use radioactive L-Dopa for monitoring of Dopa-tubulin formation within cultured cells were unsuccessful because of the low specific radioactivity, and most likely because the amount of detyrosinated tubulin was insufficient to act as L-Dopa acceptor. We were not able to generate an Ab specific to Dopa-tubulin to monitor such incorporation. As an alternative, we detected such incorporation by determining the "tyrosination state" of tubulin before and after incubation of cells in the presence of L-Dopa, that is, measurement of relative amounts of deTyr- and Tyr-tubulin (and Δ2-tubulin in some cases) relative to total-tubulin. In effect, by incorporating L-Dopa into tubulin of a soluble rat brain preparation, and determining tubulin tyrosination state, we proved that the reduction in the sum of deTyr- plus Tyr-tubulin is necessarily due to the formation of L-Dopa-tubulin. The sum of amounts of deTyr- plus Tyr-tubulin (Fig. 1) did not account for total-tubulin, whereas it did in a control preparation without L-Dopa incorporation. Although this is indirect evidence, it seems clear that Dopa-tubulin was the "missing" (new) tubulin species. These *in vitro* experiments indicate that formation of Dopa-tubulin can be determined based on reduced levels of deTyr- and/or Tyr-tubulin isospecies following incubation of cell or tissue samples with L-Dopa. Such a measurement allowed us to estimate that, after a 3-h incubation period with 500 μM L-Dopa, the resulting amount of Dopa-tubulin in cultured Neuro 2A cells was ~38% of total-tubulin (Fig. 3). These results were further verified by HPLC analysis of tubulin isolated from Neuro 2A cells that were incubated in the presence of L-Dopa (Fig. 5). The analysis showed that ~29.6% of total-tubulin contained C-terminal L-Dopa, whereas none was found in tubulin from cells incubated in the absence of L-Dopa. This value may be an underestimate, since some loss of L-Dopa may have occurred during CPA treatment and subsequent steps. In any case, these values indicate that a significant proportion of α-tubulin molecules are modified by the presence of L-Dopa at the C-terminal position. L-Dopa has a tendency to oxidize to quinone forms. However, the results presented in Fig. 5 not only indicate the amount of tubulin containing L-Dopa as C-terminal amino acid but also demonstrate that L-Dopa (not a derivative) is bound to tubulin.

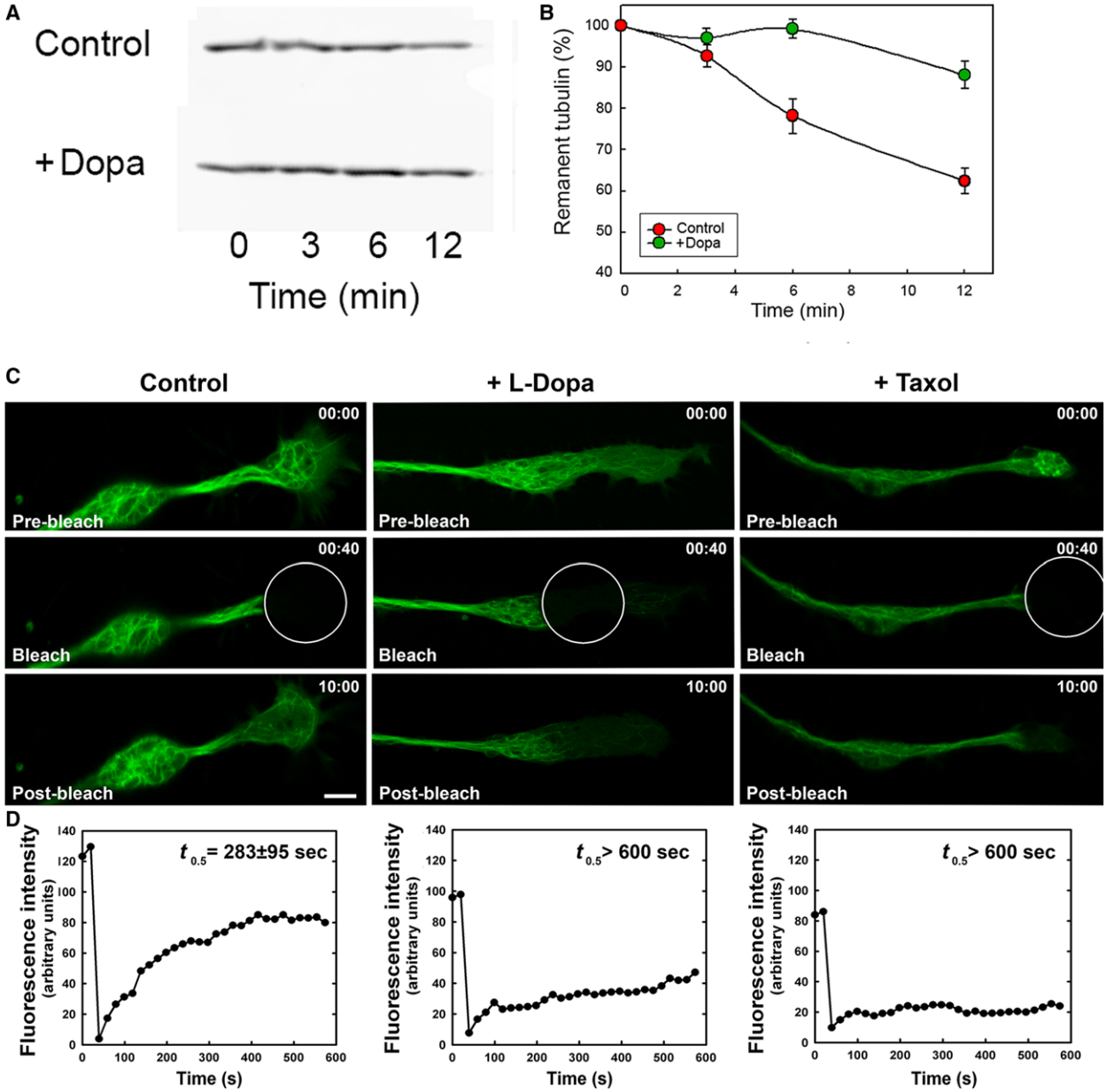

Fig. 8. Effect of L-Dopa treatment on microtubule dynamics. Differentiated CAD cells were incubated with or without L-Dopa, treated with 10 μM nocodazole for the indicated times, and processed immediately to isolate cytoskeletal fractions that remained bound to the dish (see Materials and methods). These fractions were subjected to western blotting and stained with anti-total-tubulin Ab DM1A. (A) Immunoblots corresponding to control cells (upper) and to L-Dopa-treated cells (lower) from a typical experiment. (B) O.D. values of total-tubulin are expressed as mean ± SD from three independent experiments. (C) Undifferentiated CAD cells were transfected with pEGFP-Tub and cultured under differentiating conditions for 72 h. During the last 3 h, cells were incubated in the absence (Control; left column) or presence (+L-Dopa; middle column) of 500 μM L-Dopa. As control (no microtubule dynamics), cells were incubated 10 min in the presence of 10 μM taxol (microtubule-stabilizing agent) (+ Taxol; right column). Selected fields containing growth cone-like structures not in contact with other structures were subjected to FRAP analysis (white ROI) as described in Materials and methods. Images were taken at 20-s intervals during a 10-min period after bleaching. Images representative of three replicate experiments are shown. (D) Quantification of fluorescence intensity. $t_{0.5}$ values were calculated from four independent experiments. Scale bar: 10 μm.

Findings that the capabilities of Dopa-tubulin to polymerize (Fig. 2A) and depolymerize (Fig. 2B) are similar to those of Tyr-tubulin, at least under *in vitro* condition, suggest that the new tubulin species is distributed in a uniform fashion along microtubules. This possibility was also supported by immunofluorescence

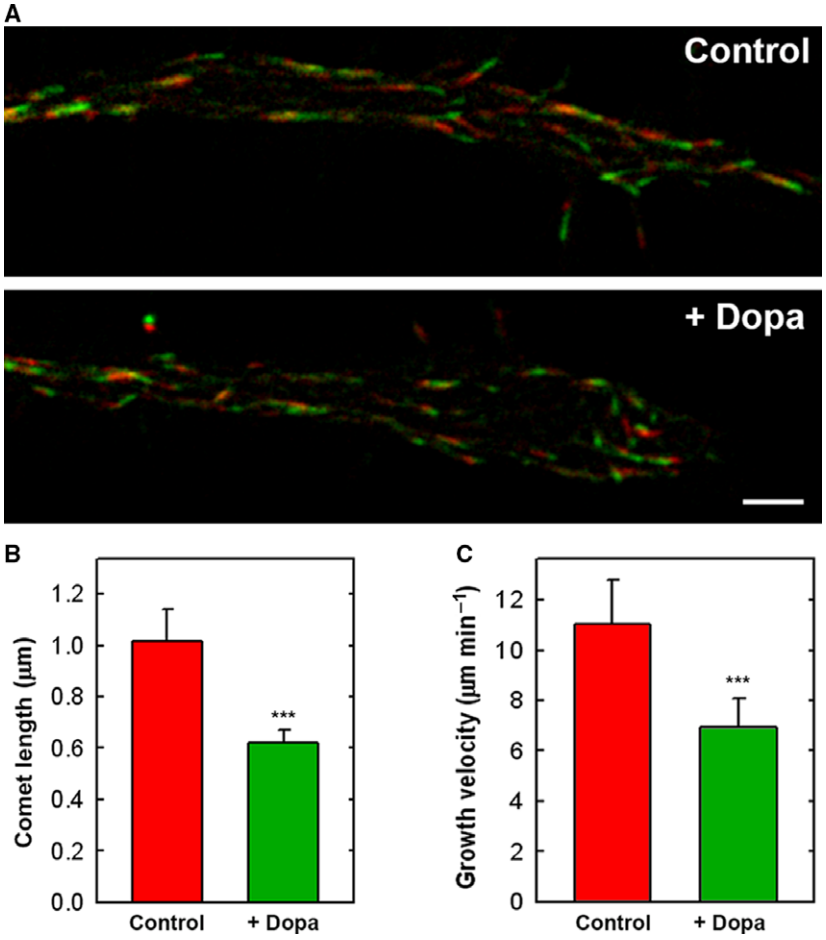

Fig. 9. Microtubule dynamics in EB3-EGFP transfected cells. Differentiated CAD cells were incubated for 1 h in the presence or absence of 500 μM L-Dopa, and images were recorded *in vivo*. (A) Overlap of three successive time-lapse images of EB3 taken at 3-s intervals. The first and third images were digitally colored red and green, respectively, to allow measurement of displacement and length of the comet tail. Top: control cells. Bottom: L-Dopa-treated cells. Scale bar: 2.5 μm. (B) For each treatment, EB3 comet tail lengths from seven cells was measured. Values represent mean length of 50 comets per cell. (C) Microtubule instantaneous growth velocities in neurite-like processes. Values represent average speed ($\mu m \cdot min^{-1}$) calculated in five cells, 30 microtubules per cell. ***$P < 0.00001$ (Student's *t*-test) for comparison of Control vs. L-Dopa treated cells. Error bars: SD.

visualization of the microtubule network before and after L-Dopa incorporation in cultured cells. DeTyr-tubulin staining declined homogeneously through the entire cell following L-Dopa incubation (Fig. 3A). The similarity of assembly/disassembly behavior of Tyr- and Dopa-tubulin observed in our *in vitro* studies could theoretically be interpreted as an irrelevant modification of microtubule function. However, the possibility cannot be ruled out that the presence of Dopa-tubulin in microtubules affects important functions such as microtubule dynamics, displacement of motor proteins, and association with microtubule-associated proteins, +TIPs, and membrane. We further investigated the possibility that L-Dopa treatment of CAD cells affects microtubule dynamics. Nocodazole treatment causes gradual depolymerization of microtubules by inhibiting the polymerization reaction, and this process is faster when microtubule dynamics is higher [27]. The finding that nocodazole-induced depolymerization in L-Dopa-treated cells is slower than that in control cells (Fig. 8A,B) suggests that L-Dopa treatment results in partial stabilization of microtubules. Direct measurement of microtubule turnover by FRAP analysis supported this concept. After bleaching of GFP-labeled microtubules, fluorescence recovery in neuron-like processes was slower for L-Dopa-treated cells than for control cells (Fig. 8C,D). Analysis of EB3 behavior in growth cone-like structures further supported the concept that L-Dopa treatment results in partial stabilization of microtubules. EB3 binds to microtubule ends to form structures that can be visualized as "comets" [23,25]. The length and speed of these structures are directly correlated with microtubule dynamics [28]. Length and instantaneous growth velocity of EB3 comets in neurite-like processes were smaller for L-Dopa-treated cells than for control cells (Fig. 9). L-Dopa treatment could conceivably affect cell functions other than microtubule dynamics; however, the observed alterations seem most likely due to L-Dopa incorporation into tubulin. Along this line, we demonstrated previously [14] that phenylalanine can be post-translationally incorporated into tubulin, and that this modification affects microtubule dynamics along with other cellular functions such as proliferation and

differentiation. The presence of only one hydroxyl group on the phenyl moiety of the C-terminal amino acid of α-tubulin appears to be essential for correct functioning of microtubules.

Microtubule dynamics is also affected by several other post-translational modifications of tubulin (acetylation, glutamylation, glycylation) [1,29]. Tubulin tyrosination state has not been previously reported to regulate dynamics; however, our present findings indicate that enhanced level of an "anomalous" tubulin isospecies may alter interactions with various proteins involved in regulation of microtubule functions. In this regard, the high concentrations of L-Dopa sometimes administered to Parkinson's disease patients could conceivably result in incorporation of this amino acid into tubulin and formation of Dopa-tubulin-enriched microtubules, perhaps leading to dysfunction of such microtubules which could be related with some of the symptoms observed in Levodopa-induced dyskinesia. This possibility is being addressed in our ongoing studies. CAD cells are particularly suitable for these studies because they are derived from a dopaminergic area of mouse brain [20], differentiate to neuron-like morphology, and display many characteristics of neurons under defined culture conditions [30]. Large amounts of L-Dopa can be incorporated into tubulin of differentiated CAD cells without notable cell injury (Fig. 7). This cell system, therefore, provides a simple, reliable model for studying effects of Dopa-tubulin formation on neural physiology.

Materials and methods

Chemicals

Unless otherwise stated, chemicals and culture media were from Sigma-Aldrich, USA. L-[U-^{14}C]Tyr (specific activity 464 mCi·mmol^{-1}), L-[2,3,5,6-^{3}H]Tyr (specific activity 96 Ci/mmol), and L-3,4-dihydroxyphenyl[3-^{14}C]alanine (specific activity 55 mCi·mmol^{-1}) were from Amersham Pharmacia Biotech, UK. Tolcapone was kindly provided by P. Soares-da-Silva, Dept. of Pharmacology and Therapeutics, Faculty of Medicine, Porto, Portugal. FBS was from Natocor (Córdoba, Argentina). Y-27632 and FluorSave were from Calbiochem (Billerica, MA, USA).

Antibodies

Rabbit polyclonal antibodies (Abs) specific to deTyr-tubulin (anti-deTyr) and Δ2-tubulin (anti-Δ2) were prepared in our laboratory as described previously [31]. Mouse monoclonal Abs against Tyr-tubulin (Tub 1A2) and total-α-tubulin (DM1A) were from Sigma-Aldrich. Secondary Abs IRDye 800CW goat anti-mouse IgG and IRDye 800CW goat anti-rabbit IgG were from Li-Cor Biosciences (Lincoln, NE, USA). Alexa 488 and Alexa 546 were from Thermo Fisher-Invitrogen (Waltham, MA, USA).

Rat brain soluble extract

Brains from 15- to 30-day-old Wistar rats were homogenized in one volume (w/v) MEM buffer (100 mM Mes adjusted with NaOH to pH 6.7, containing 1 mM EGTA and 1 mM $MgCl_2$). The homogenate was centrifuged at 100 000 *g* for 1 h at 4 °C, and supernatant solution was passed, as indicated, through a column of Sephadex G-25-80 equilibrated with MEM buffer to eliminate low molecular weight compounds. Protein concentration in this preparation was ~ 13 mg·mL^{-1}. This was assumed to correspond to tubulin concentration ~ 1.95 mg·mL^{-1} (18 nmol·mL^{-1} of tubulin), on the basis of previous reports that tubulin represents ~ 15% of total proteins in such brain preparations [15].

In vitro incorporation of L-Tyr and L-Dopa into tubulin

The incubation medium was composed of (per mL) 0.9 mL soluble brain extract passed through Sephadex G-25, 2.5 μmol ATP, 12.5 μmol $MgCl_2$, 30 μmol KCl, 100 μmol Mes buffer (pH 6.7), and 2 μCi (0.3 μmol) [^{14}C]Tyr or 3 μCi (0.3 μmol) [^{14}C]Dopa. For L-Dopa incorporation, 12 mM ascorbic acid was included. Incubation temperature was 37 °C. When indicated, 50-μL aliquots were removed and inactivated by addition of 2 mL 5% trichloroacetic acid and heating (90 °C for 15 min). Radioactivity bound to protein was measured in hot TCA-insoluble material as described previously [17]. Radioactive Tyr-tubulin and Dopa-tubulin, for use as substrates of tubulin carboxypeptidase and for determination of assembly and disassembly capabilities, were prepared as described above except for changes in the radioactive isotope and the specific activity of radioactive amino acids in the incubation system, depending on the particular experiment.

Determination of the capability of Dopa-tubulin and Tyr-tubulin to assemble into and to disassemble from microtubules

[^{3}H]Tyr and [^{14}C]Dopa were incorporated in parallel into tubulin of soluble rat brain extracts, the incubation mixtures were cooled to 0 °C and passed through Sephadex G-25 columns equilibrated with MEM buffer, and eluted proteins were combined. This preparation was added with two volumes of a corresponding soluble brain preparation not passed through Sephadex. The mixture was incubated at 37 °C under assembly conditions (0.2 mM GTP, 40% glycerol) for 10, 20, or 30 min (to measure assembly capability), and then centrifuged at 100 000 *g* for 10 min at

27 °C. Radioactivity bound to protein was measured in aliquots of supernatant and resuspended pellet fractions.

To measure disassembly capability, two identical samples containing mixed [^{14}C]Dopa-tubulin and [^{3}H]Tyr-tubulin were incubated under assembly conditions for 30 min as described above. One sample was immediately centrifuged for 15 min at 27 °C to separate assembled (P) and nonassembled (SN) tubulin fractions. The other sample was diluted by the addition of nine volumes of cold MEM buffer, kept at 0 °C for 30 min with gentle stirring, and then centrifuged for 15 min at 2–4 °C. Radioactivity bound to the protein was measured in supernatant and pellet fractions. Values (mean ± SD from four independent experiments) are expressed as percent radioactivity in each fraction relative to sum of radioactivity in both fractions.

Cell culture

Neuro 2A, C6, CHO, and COS cells were cultured in Dulbecco's modified Eagle's medium (DMEM), and CAD cells were cultured in DMEM/F12 (50 : 50, v/v). Both media were supplemented with 10% (v/v) FBS, 10 units·mL^{-1} penicillin, and 100 μg·mL^{-1} streptomycin. Cultured cells were maintained at 37 °C in a humidified 5% CO_2 atmosphere. Differentiation of CAD cells was induced by replacement of medium with FBS-free medium, and differentiation status (neurite growth) was assessed by optical microscopic examination.

Incorporation of L-Dopa into tubulin in cultured cells

L-Dopa was incorporated into cultured cells as described previously [18]. In brief, culture medium was removed and cells were washed twice with modified Hank's balanced salt solution (mHBSS) (137 mM NaCl, 5 mM KCl, 0.8 mM $MgSO_4$, 0.33 mM Na_2HPO_4, 0.44 mM KH_2PO_4, 0.25 mM $CaCl_2$, 1 mM $MgCl_2$, 0.15 mM Tris-HCl, freshly prepared 1 mM sodium butyrate, 50 μM Carbidopa, and 1 μM tolcapone; final pH = 7.4). Carbidopa and tolcapone were added to inhibit enzyme activities of aromatic L-amino acid decarboxylase (AADC) and catechol-O-methyltransferase (COMT), respectively. Cells were washed, incubated in mHBSS (37 °C; 5% CO_2 atmosphere) for 30 min, and medium was renewed with fresh mHBSS with or without 500 μM L-Dopa. Cells were incubated in the dark for 3 h, medium was removed, cells were harvested in sample buffer [32], and proteins were subjected to electrophoresis and western blotting as described below.

Identification and quantitation of the compound bound to α-tubulin C terminus after incubation of cells with L-Dopa

At the end of incubation for L-Dopa incorporation as described above, Neuro 2A cells were harvested in Laemmli buffer, separated by SDS/PAGE, and transferred to nitrocellulose sheets. The nitrocellulose area corresponding to tubulin was cut out and incubated in a minimum volume with 100 μg·mL^{-1} pancreatic carboxypeptidase A (CPA) (52 U·mg^{-1}) to remove the C-terminal residue from tubulin. The liquid phase was collected, concentrated by lyophilization, resuspended in a small volume, and an aliquot was analyzed by HPLC using a reverse-phase column (Zorbax SB C18, 4.6 × 150 mm, 3.5 μm; Agilent Technologies, Santa Clara, CA, USA). Mobile phase: acetonitrile/water (10 : 100) containing 0.01% EDTA-Na_2, 0.01% NaCl, 0.02% sodium 1-octanesulfonate, pH adjusted to 3.2. Isocratic flow: 0.8 mL·min^{-1}. Potentials: E1: +400 mV; E2: −200 mV, with a guard cell potential of +300 mV. Injection volume: 20 μL. Peak heights were measured using an HP 1100 ChemStation (Agilent Technologies). A control corresponding to cells incubated in the absence of L-Dopa was run in parallel.

Determination of cell viability

The effect of L-Dopa on cellular proliferation/viability was determined by 3-(4,5-dimethylthiazol-2-yl)-2,5-diphenyltetrazolium bromide (MTT) assay. CAD cells were seeded in 96-well plates in 100 μL medium (density 5000 cells/well), left to attach overnight, incubated with mHBSS for 30 min, and then incubated with 500 μM L-Dopa in mHBSS (or vehicle alone) for 3 h. In one set of experiments, cells were incubated immediately after L-Dopa treatment with MTT reagent (final concentration 5 mg·mL^{-1}) for 4 h, intracellular formazan crystals were solubilized with 100 μL isopropanol, and absorbance at 490 nm was measured by an ELISA plate reader. In a second set of experiments, cells were incubated after L-Dopa treatment for 24 h in DMEM/F12 medium with 10% FBS without L-Dopa, and MTT assay was performed. For each treatment group, number of cells was expressed as percentage relative to cells treated with vehicle alone. All experiments were performed in triplicate.

Immunofluorescence assay

Cells were cultured on coverslips, fixed with NaCl/Pi containing 4% paraformaldehyde and 3% sucrose for 10 min, permeabilized with NaCl/Pi containing 0.25% Triton X-100, washed with NaCl/Pi, incubated 1 h with 5% (w/v) BSA in NaCl/Pi, incubated with primary Ab 4 h at 37 °C, washed three times with NaCl/Pi, and incubated 1 h at 37 °C with Alexa 488 anti-mouse IgG and Alexa 594 (Life Technologies, Carlsbad, CA, USA), both at 1 : 2000 dilution. Coverslips were mounted in FluorSave (Calbiochem, San Diego, CA, USA), and fluorescence was observed by confocal microscopy (FluoView 1000; Olympus, Tokyo, Japan). For comparison of different preparations, photographs were taken using the same gain value.

Electrophoresis and western blotting

Proteins were separated by SDS/PAGE (10% gels), and transferred to nitrocellulose sheets. Blots were incubated with primary Abs (anti-total-, 1 : 1000; anti-Tyr-, 1 : 1000; anti-deTyr-, 1 : 200; anti-Δ2-tubulin, 1 : 400), and then incubated with infrared fluorescent secondary Abs (1 : 20 000). Sheets were scanned using an Odyssey infrared scanner (Li-Cor Bioscience), and O.D. of bands were quantitated using the SCION IMAGE software (Scion Corp., Houston, TX, USA).

Nocodazole assay

Differentiated CAD cells were incubated in mHBSS for 1 h in the presence or absence of 500 μM L-Dopa, treated with 10 μM nocodazole for various times (0, 3, 6, 12 min), and immediately processed to isolate cytoskeletal fraction as described previously [33]. Cytoskeletons remaining attached to dishes were washed twice with 5 mL prewarmed microtubule-stabilizing buffer, subjected to SDS/PAGE and western blotting, and revealed with anti-total-tubulin Ab.

Fluorescence recovery after photobleaching analysis

Undifferentiated CAD cells were grown to 80% confluence in a microslide glass-bottom chamber (Ibidi; Martinsried, Germany), transfected with pEGFP-Tub (Clontech; Mountain View, CA, USA) according to the manufacturer's protocol, grown for 72 h under differentiating conditions, incubated (or not) with L-Dopa as described above, and subjected to FRAP analysis, that is, photobleaching of GFP-tubulin in a defined area of the cell, followed by measurement of fluorescence recovery in this area as a function of time. Fluorescence values were also measured in a background region, as control. Five to seven growth cone-like structures were analyzed for each experimental condition. Before and after photobleaching, images were acquired every 20 s during a 10-min period, using a 20 × 0.5 numerical aperture objective (Plan-Neofluar, Carl Zeiss, Oberkochen, Germany) with confocal pinhole of microscope fully open. Selective photobleaching of GFP was performed under a laser-scanning confocal microscope (FluoView 1000, Olympus). During image acquisition, living cells were maintained at 37 °C in 5% CO_2 atmosphere. Fluorescence in selected regions of interest was quantitated using the Fiji processing package of the IMAGEJ program (National Institutes of Health; Bethesda, MD, USA).

Microtubule dynamics assay following transfection with EB3-EGFP

The CAD cells were transfected with EB3-EGFP plasmid (kindly provided by Dr. Mariano Bisbal, Instituto de Investigación Médica Mercedes y Martín Ferreyra, Cordoba, Argentina) using Lipofectamine LTX reagent (ThermoFisher Scientific) according to the manufacturer's protocol, and 24 h later were treated with 500 μM L-Dopa as described above. Medium was replaced with DMEM/F12, and cells were examined by microscopy. Because EB3 promotes microtubule stabilization, only cells with low levels of EB3-EGFP expression were analyzed. Time-lapse recordings of transfected cells were performed at 3-s intervals during 5 min with a laser-scanning confocal microscope (FluoView 1200, Olympus). During image acquisition, living cells were maintained at 37 °C in 5% CO_2 atmosphere. Comet length and velocity were quantitated using Fiji.

For measurement of microtubule instantaneous growth velocity, we analyzed five image stacks recorded from five different cells for each treatment. For each stack, at five different time points, three successive images were merged. The first and third images were digitally colored red and green, respectively, so that displacement of microtubule tips could be measured. Growth velocity was calculated as the displacement (in μm) divided by elapsed time (6 s). Growth velocity was measured for at least six microtubules per time point selected (at least 30 measurements per cell). For comet length measurements, six random images were selected from each image stack obtained from five different cells.

Microscopy facilities

All microscopic observations, including those for FRAP analysis, were performed at the Centro de Microscopía Óptica y Confocal de Avanzada (CIQUIBIC-CONICET; Córdoba, Argentina).

Acknowledgements

This study was supported by the Agencia Nacional de Promoción Científica y Tecnológica de la Secretaria de Ciencia y Tecnología del Ministerio de Cultura y Educación (Prestamo BID-PICT 0826), the Consejo Nacional de Investigaciones Científicas y Técnicas (CONICET), and the Secretaria de Ciencia y Técnica de la Universidad Nacional de Córdoba. The authors are grateful to Dr. S. Anderson for English editing of the manuscript.

Conflict of interest

The authors declare no competing financial interests.

Author contributions

The experiments were designed by YD, CAA, and CGB, and performed by YMD, YD, and CGB. HPLC

measurements and data analysis were performed by CH, YD, CAA, and CGB analyzed the data, wrote the manuscript, and assume primary responsibility for the final content. All the authors read and approved the final manuscript.

References

1 Barra HS, Arce CA & Argarana CE (1988) Posttranslational tyrosination/detyrosination of tubulin. *Mol Neurobiol* **2**, 133–153.

2 Janke C & Bulinski JC (2011) Post-translational regulation of the microtubule cytoskeleton: mechanisms and functions. *Nat Rev Mol Cell Biol* **12**, 773–786.

3 Rogowski K, van Dijk J, Magiera MM, Bosc C, Deloulme JC, Bosson A, Peris L, Gold ND, Lacroix B, Bosch Grau M *et al*. (2010) A family of protein-deglutamylating enzymes associated with neurodegeneration. *Cell* **143**, 564–578.

4 Tort O, Tanco S, Rocha C, Bieche I, Seixas C, Bosc C, Andrieux A, Moutin MJ, Aviles FX, Lorenzo J *et al*. (2014) The cytosolic carboxypeptidases CCP2 and CCP3 catalyze posttranslational removal of acidic amino acids. *Mol Biol Cell* **25**, 3017–3027.

5 Barra HS, Arce CA & Caputto R (1980) Total tubulin and its aminoacylated and non-aminoacylated forms during the development of rat brain. *Eur J Biochem* **109**, 439–446.

6 Paturle-Lafanechere L, Edde B, Denoulet P, Van Dorsselaer A, Mazarguil H, Le Caer JP, Wehland J & Job D (1991) Characterization of a major brain tubulin variant which cannot be tyrosinated. *Biochemistry* **30**, 10523–10528.

7 Rovini A, Gauthier G, Berges R, Kruczynski A, Braguer D & Honore S (2013) Anti-migratory effect of vinflunine in endothelial and glioblastoma cells is associated with changes in EB1 C-terminal detyrosinated/tyrosinated status. *PLoS One* **8**, e65694.

8 Bosson A, Soleilhac JM, Valiron O, Job D, Andrieux A & Moutin MJ (2012) Cap-Gly proteins at microtubule plus ends: is EB1 detyrosination involved? *PLoS One* **7**, e33490.

9 Barisic M, Silva e Sousa R, Tripathy SK, Magiera MM, Zaytsev AV, Pereira AL, Janke C, Grishchuk EL & Maiato H (2015) Mitosis. Microtubule detyrosination guides chromosomes during mitosis. *Science* **348**, 799–803.

10 Song Y & Brady ST (2015) Post-translational modifications of tubulin: pathways to functional diversity of microtubules. *Trends Cell Biol* **25**, 125–136.

11 Barisic M & Maiato H (2016) The tubulin code: a navigation system for chromosomes during mitosis. *Trends Cell Biol* **26**, 766–775.

12 Peris L, Wagenbach M, Lafanechere L, Brocard J, Moore AT, Kozielski F, Job D, Wordeman L & Andrieux A (2009) Motor-dependent microtubule disassembly driven by tubulin tyrosination. *J Cell Biol* **185**, 1159–1166.

13 Peris L, Thery M, Faure J, Saoudi Y, Lafanechere L, Chilton JK, Gordon-Weeks P, Galjart N, Bornens M, Wordeman L *et al*. (2006) Tubulin tyrosination is a major factor affecting the recruitment of CAP-Gly proteins at microtubule plus ends. *J Cell Biol* **174**, 839–849.

14 Ditamo Y, Dentesano YM, Purro SA, Arce CA & Bisig CG (2016) Post-translational incorporation of L-phenylalanine into the C-terminus of alpha-tubulin as a possible cause of neuronal dysfunction. *Sci Rep* **6**, 38140.

15 Arce CA, Rodriguez JA, Barra HS & Caputo R (1975) Incorporation of L-tyrosine, L-phenylalanine and L-3,4-dihydroxyphenylalanine as single units into rat brain tubulin. *Eur J Biochem* **59**, 145–149.

16 Purro SA, Bisig CG, Contin MA, Barra HS & Arce CA (2003) Post-translational incorporation of the antiproliferative agent azatyrosine into the C-terminus of alpha-tubulin. *Biochem J* **375**, 121–129.

17 Bisig CG, Purro SA, Contin MA, Barra HS & Arce CA (2002) Incorporation of 3-nitrotyrosine into the C-terminus of alpha-tubulin is reversible and not detrimental to dividing cells. *Eur J Biochem* **269**, 5037–5045.

18 Sampaio-Maia B & Soares-da-Silva P (2000) Ca2+/calmodulin mediated pathways regulate the uptake of L-DOPA in mouse neuroblastoma neuro 2A cells. *Life Sci* **67**, 3209–3220.

19 Contin MA, Purro SA, Bisig CG, Barra HS & Arce CA (2003) Inhibitors of protein phosphatase 1 and 2A decrease the level of tubulin carboxypeptidase activity associated with microtubules. *Eur J Biochem* **270**, 4921–4929.

20 Qi Y, Wang JK, McMillian M & Chikaraishi DM (1997) Characterization of a CNS cell line, CAD, in which morphological differentiation is initiated by serum deprivation. *J Neurosci* **17**, 1217–1225.

21 Chesta ME, Carbajal A, Arce CA & Bisig CG (2014) Serum-induced neurite retraction in CAD cells–involvement of an ATP-actin retractile system and the lack of microtubule-associated proteins. *FEBS J* **281**, 4767–4778.

22 Zilberman Y, Ballestrem C, Carramusa L, Mazitschek R, Khochbin S & Bershadsky A (2009) Regulation of microtubule dynamics by inhibition of the tubulin deacetylase HDAC6. *J Cell Sci* **122**, 3531–3541.

23 Akhmanova A & Hoogenraad CC (2005) Microtubule plus-end-tracking proteins: mechanisms and functions. *Curr Opin Cell Biol* **17**, 47–54.

24 Ramirez-Rios S, Denarier E, Prezel E, Vinit A, Stoppin-Mellet V, Devred F, Barbier P, Peyrot V, Sayas CL, Avila J *et al.* (2016) Tau antagonizes end-binding protein tracking at microtubule ends through a phosphorylation-dependent mechanism. *Mol Biol Cell* **27**, 2924–2934.
25 Galjart N (2010) Plus-end-tracking proteins and their interactions at microtubule ends. *Curr Biol* **20**, R528–R537.
26 Rodriguez JA, Barra HS, Arce CA, Hallak ME & Caputto R (1975) The reciprocal exclusion by L-dopa (L-3,4-dihydroxyphenylalanine) and L-tyrosine of their incorporation as single units into a soluble rat brain protein. *Biochem J* **149**, 115–121.
27 Vasquez RJ, Howell B, Yvon AM, Wadsworth P & Cassimeris L (1997) Nanomolar concentrations of nocodazole alter microtubule dynamic instability in vivo and in vitro. *Mol Biol Cell* **8**, 973–985.
28 Kleele T, Marinkovic P, Williams PR, Stern S, Weigand EE, Engerer P, Naumann R, Hartmann J, Karl RM, Bradke F *et al.* (2014) An assay to image neuronal microtubule dynamics in mice. *Nat Commun* **5**, 4827.
29 Wloga D & Gaertig J (2010) Post-translational modifications of microtubules. *J Cell Sci* **123**, 3447–3455.
30 Li Y, Hou LX-E, Aktiv A & Dahlström A (2007) Studies of the central nervous system-derived CAD cell line, a suitable model for intraneuronal transport studies? *J Neurosci Res* **85**, 2601–2609.
31 Gundersen GG, Kalnoski MH & Bulinski JC (1984) Distinct populations of microtubules: tyrosinated and nontyrosinated alpha tubulin are distributed differently in vivo. *Cell* **38**, 779–789.
32 Laemmli UK (1970) Cleavage of structural proteins during the assembly of the head of bacteriophage T4. *Nature* **227**, 680–685.
33 Bisig CG, Chesta ME, Zampar GG, Purro SA, Santander VS & Arce CA (2009) Lack of stabilized microtubules as a result of the absence of major maps in CAD cells does not preclude neurite formation. *FEBS J* **276**, 7110–7123.

Supporting information

Additional Supporting Information may be found online in the supporting information tab for this article:
Movie S1. Fluorescence recovery after photobleaching (FRAP) in vehicle-treated (control) CAD cells.
Movie S2. FRAP in L-Dopa-treated CAD cells.
Movie S3. FRAP in taxol-treated CAD cells.